Journal of Sound and Vibration (1997) **201**(2), 272–280

DECOUPLING LONGITUDINAL AND TRANSVERSE VIBRATIONS OF A CYLINDRICAL BEAM IN TIME AND FREQUENCY DOMAINS

R. SUN, F. OTUONYE, C. VAN KARSEN AND J. LIGON
College of Engineering, Michigan Technological University, Houghton, MI 49931, *U.S.A.*

(*Received* 1 *July* 1996, *and in final form* 23 *July* 1996)

1. INTRODUCTION

In the vibration analysis of structural systems under a combination of longitudinal and transverse loads, it often becomes necessary to study the dynamic behavior of longitudinal vibration and transverse vibration of the structure separately. This requires decoupling the longitudinal vibration and transverse vibration from each other when the two are present in the data. Strictly speaking, neither pure transverse nor pure longitudinal vibration exists in a practical case. They are almost always combined with each other or some other components, such as torsion and shearing, depending on the loading conditions and the mechanical and geometrical properties of the structure. By decoupling these two types of vibrations from the original measurements of the structure, it helps us to understand the contribution and significance of each component to the total response of the structure. Also, decoupling makes it possible to evaluate the dynamic behavior of longitudinal and transverse vibrations of the structure separately. Considering that vibration analysis can be conducted in both time domain and frequency domain, decoupling the two components in the two domains can be very useful in the dynamic analysis of the structure.

In this paper, by using strain gage techniques, an approach to decouple the longitudinal vibration and transverse vibration of a cylindrical beam in both time and frequency domains is discussed. The relevant equations are developed and applied to a case of a cylindrical beam excited by an eccentric axial impact load.

2. EQUATIONS FOR DECOUPLING

In the case of static loading, Tuttle [1] proposed that, using three uniaxial strain gages (A, B and C) mounted parallel to the axis of a cylindrical column and 120° apart (Figure 1), the axial load, P, can be determined for the cylindrical beam by using equation (1):

$$P = (AE/3)(\varepsilon_A + \varepsilon_B + \varepsilon_C), \tag{1}$$

where P = axial load on the beam, N; A = cross-sectional area of the beam, m^2; E = Young's modulus of the material, N/m^2; ε_A, ε_B, and ε_C are strain levels recorded individually at the same load level from strain gages A, B, and C, respectively.

From equation (1), the axial strain, ε_l, can be expressed as

$$\varepsilon_l = \tfrac{1}{3}(\varepsilon_A + \varepsilon_B + \varepsilon_C). \tag{2}$$

Equation (2) indicates that the axial strain at the cross-section of measurement point is the average of the readings from the three strain gages. Assuming that the measured strains are composed of two components, namely, axial strain and bending strains, then

$$\epsilon_i = \epsilon_l + \epsilon_{ti}, \tag{3}$$

0022–460X/97/120272 + 09 $25.00/0/dv960737

where ε_i is the measured strain from gage $i =$ A, B, C; ε_l is the axial strain at measurement point; ε_{ti} is the bending strain at measurement point $i =$ A, B, C. Hence, once the axial strain, ε_l, is obtained from the measurements by using equation (2), the bending strain, ε_{ti}, can be calculated accordingly by using equation (3) as

$$\varepsilon_{ti} = \varepsilon_i - \varepsilon_l. \tag{4}$$

Similarly, in the case of dynamic loading, the same approach can be directly applied to time domain analysis. The only difference is that the strains in the dynamic case are functions of time.

For a cylindrical beam in elastic stability and subjected to longitudinal and transverse vibrations, the total strain signal at the measured site can be expressed as

$$\varepsilon_i(t) = \varepsilon_l(t) + \varepsilon_{ti}(t), \qquad \varepsilon_l(t) = \tfrac{1}{3}[\varepsilon_A(t) + \varepsilon_B(t) + \varepsilon_C(t)], \qquad \varepsilon_{ti}(t) = \varepsilon_i(t) - \varepsilon_l(t), \quad (5\text{–}7)$$

where $\varepsilon_i(t)$ is the measured strain signal from gage $i =$ A, B, C; $\varepsilon_l(t)$ is the longitudinal strain at measurement site; $\varepsilon_{ti}(t)$ is the transverse strain at measurement site $i =$ A, B, C; $\varepsilon_A(t)$, $\varepsilon_B(t)$ and $\varepsilon_C(t)$, are strain signals recorded simultaneously from strain gages A, B and C, respectively. Therefore, once the longitudinal vibration $\varepsilon_l(t)$, is obtained from the measurements by using equation (6), the component of transverse vibration, $\varepsilon_{ti}(t)$, can be calculated accordingly by using equation (7). Then, the longitudinal and transverse vibrations of a cylindrical beam can be decoupled in the time domain by using equations (6) and (7).

In the frequency domain, considering that the Fourier transform is a linear operation [2], and by taking the Fourier transform of both sides of equation (6), one obtains

$$\mathscr{F}[\varepsilon_l(t)] = \tfrac{1}{3}\mathscr{F}[\varepsilon_A(t) + \varepsilon_B(t) + \varepsilon_C(t)] = \tfrac{1}{3}\{\mathscr{F}[\varepsilon_A(t)] + \mathscr{F}[\varepsilon_B(t)] + \mathscr{F}[\varepsilon_C(t)]\}. \tag{8}$$

Therefore,

$$\varepsilon_l(\omega) = \tfrac{1}{3}[\varepsilon_A(\omega) + \varepsilon_B(\omega) + \varepsilon_C(\omega)], \tag{9}$$

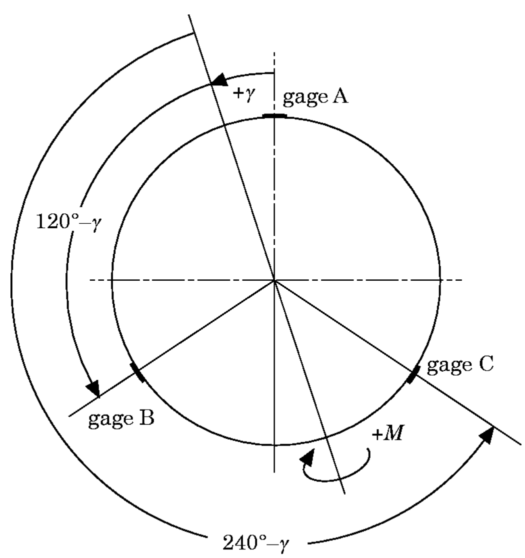

Figure 1. Layout of the strain gages on a cylindrical beam [1]. M is the bending moment; γ is the angle between the neutral axis and the nearest gage; Positive axial load P acts perpendicular to and out from the figure.

where $\mathscr{F}$ is the Fourier transform operator; $\varepsilon_l(\omega)$ is the linear spectrum of the longitudinal strain at measurement site; $\varepsilon_A(\omega)$, $\varepsilon_B(\omega)$, and $\varepsilon_C(\omega)$ are the linear spectra of measured strain signal at gages A, B, and C, respectively.

Let $H_A(\omega)$, $H_B(\omega)$ and $H_C(\omega)$ be the frequency response function (FRF) between the strain $\varepsilon_A(t)$, $\varepsilon_B(t)$ and $\varepsilon_C(t)$ and the input forces, $f(t)$, at the measurement site, respectively. Then from the definition of FRF [5], one has

$$H_A(\omega) = \varepsilon_A(\omega)/F(\omega), \qquad H_B(\omega) = \varepsilon_B(\omega)/F(\omega), \qquad H_C(\omega) = \varepsilon_C(\omega)/F(\omega). \tag{10}$$

Then,

$$\varepsilon_A(\omega) = H_A(\omega)F(\omega), \qquad \varepsilon_B(\omega) = H_B(\omega)F(\omega), \qquad \varepsilon_C(\omega) = H_C(\omega)F(\omega).$$

Then, from equation (10),

$$\varepsilon_l(\omega) = \tfrac{1}{3}[H_A(\omega) + H_B(\omega) + H_C(\omega)]F(\omega) \tag{11}$$

and

$$H_l(\omega) = \varepsilon_l(\omega)/F(\omega) = \tfrac{1}{3}[H_A(\omega) + H_B(\omega) + H_C(\omega)], \tag{12}$$

where $H_l(\omega)$ is the FRF between the longitudinal strain vibration, $\varepsilon_l(t)$, and the input force, $f(t)$; $F(\omega) = \mathscr{F}[f(t)]$ is the linear spectrum of the input force, $f(t)$.

Similarly, taking the Fourier transform of both sides of equation (6) gives

$$\mathscr{F}[\varepsilon_t(t)] = \mathscr{F}[\varepsilon_i(t) + \varepsilon_l(t)] = \mathscr{F}[\varepsilon_i(t)] + \mathscr{F}[\varepsilon_l(t)].$$

Then,

$$\varepsilon_{ti}(\omega) = \varepsilon_i(\omega) - \varepsilon_l(\omega), \qquad H_{ti}(\omega) = \varepsilon_{ti}(\omega)/F(\omega) = H_i(\omega) - H_l(\omega), \tag{13, 14}$$

where $\varepsilon_i(\omega)$ is the linear spectrum of measured strain signal from gage $i = \text{A, B, and C}$; $\varepsilon_{ti}(\omega)$ is the linear spectrum of transverse strains at gage $i = \text{A, B, and C}$; $H_i(\omega)$ is the FRF measurement from gage $i = \text{A, B, and C}$; $H_{ti}(\omega)$ is the FRF of transverse strains at gage $i = \text{A, B, and C}$.

By using equations (12) and (14), the FRF between the longitudinal and transverse vibration of a cylindrical beam at the measurement site and the input force can be decoupled from the FRF measurements at three strain gages.

3. DECOUPLING LONGITUDINAL AND TRANSVERSE VIBRATIONS IN THE FREQUENCY DOMAIN

In order to investigate the validity of the above approach, equation (12) and (14) were applied to the vibration analysis of a long cylindrical steel beam under impact excitation [3, 4]. One end of the beam was anchored in a concrete block and the other end was tightened against another concrete block (Figure 2) by torquing to 27 N m. The geometric and mechanical properties of the beam are shown in Table 1. In total, nine strain gages of 350 Ω and 0·32 cm gage length were bonded at three locations longitudinally along the beam. At each measurement site, three gages were mounted 120° apart (Figure 1). All gages were bonded in place with a strain gage adhesive. At each location, the strain response from each gage, ε_A, ε_B and ε_C, was captured individually at the same time. A system with an internal quarter bridge was used to measure the strain signals from the instrumented beam. Excitation (Figure 3) was applied to the beam longitudinally and eccentrically at the end of the beam with an impact hammer. The strain time history and FRF at each gage were measured simultaneously. All signals were recorded with a digital spectrum analyzer.

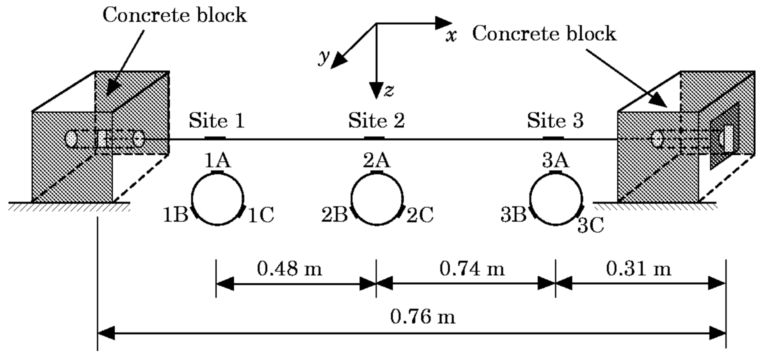

Figure 2. Sketch of experimental setup.

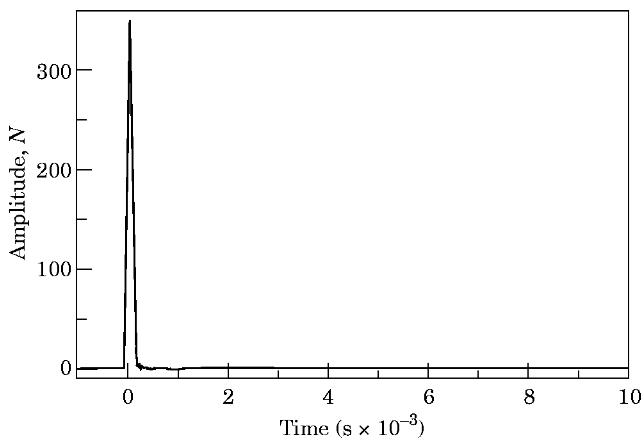

Figure 3. Impact force time history.

With this test set-up and excitation approach, the torsional vibration of the beam was not excited. Obviously, due to the slenderness of the beam and the eccentricity of the impact force, the transverse vibration is always excited and coupled with the longitudinal vibration. Based on the FRF measurements from each gage, and using equations (12) and (14), the FRF of longitudinal vibration at each measurement site and the FRF of transverse vibration at each gage can be extracted from the data. Figures 4–6 show the FRFs between the longitudinal vibration at each measurement site and the impact force, decoupled from the FRF measurements by using equation (12). It is shown that, after decoupling, most of the peaks in the original FRF are cancelled. However, in order to be sure that the decoupled FRFs are longitudinal FRF, those cancelled peaks must be shown to belong to the transverse vibration of the beam. For this purpose, the measured strain

Table 1

Geometric and mechanical properties of the beam

length (m)	diameter (m)	Young's modulus (N/m^2)	Moment of inertia (m^4)	Section area (m^2)	Mass density (kg/m^2)
1·76	0·014	$20{\cdot}34 \times 10^{10}$	$2{\cdot}05 \times 10^{-9}$	$1{\cdot}61 \times 10^{-4}$	$7{\cdot}69 \times 10^{-3}$

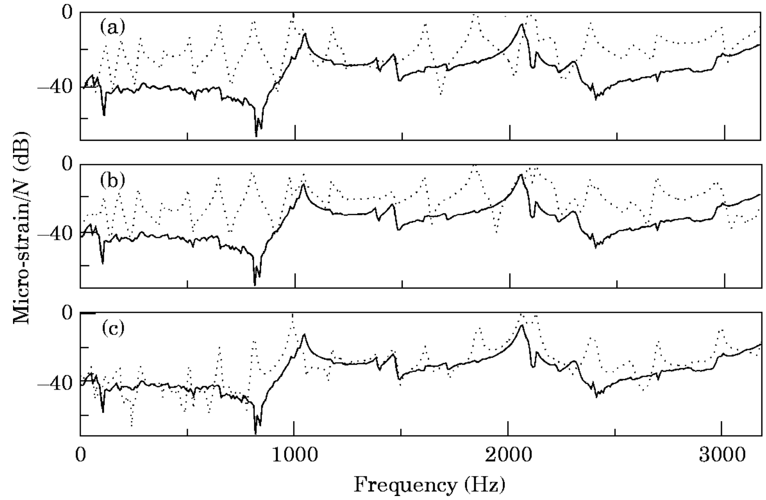

Figure 4. Decoupled FRF of longitudinal vibration at site 1. (a) Gage 1A, (b) gage 1B, (c) gage 1C; . . . . , before decoupling; ——, after decoupling.

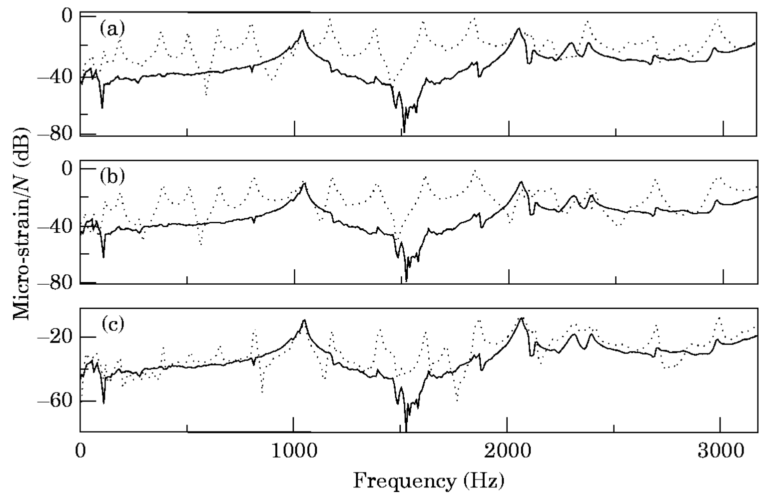

Figure 5. Decoupled FRF of longitudinal vibration at site 2. (a) Gage 2A, (b) gage 2B, (c) gage 2C; . . . . , before decoupling; ——, after decoupling.

FRF at gage 1A was digitized at each cancelled peak. Comparison (Table 2) between the digitized results and the measured transverse frequencies [3] shows that all the cancelled peaks belong to the transverse component. These results illustrated that, by using equation (12), the FRF of longitudinal vibration can be decoupled from the measurements with a high degree of precision.

TABLE 2

Comparison of cancelled peaks with transverse frequencies

Mode no.	1	2	3	4	5	6	7	8	9
Cancelled peaks (Hz)	27·7	58·2	119·1	188·4	279·8	390·6	512·5	656·5	817·2
Transverse frequency (Hz)	27·2	63·4	119·3	188·4	277·9	389·3	510·5	656·4	816·6

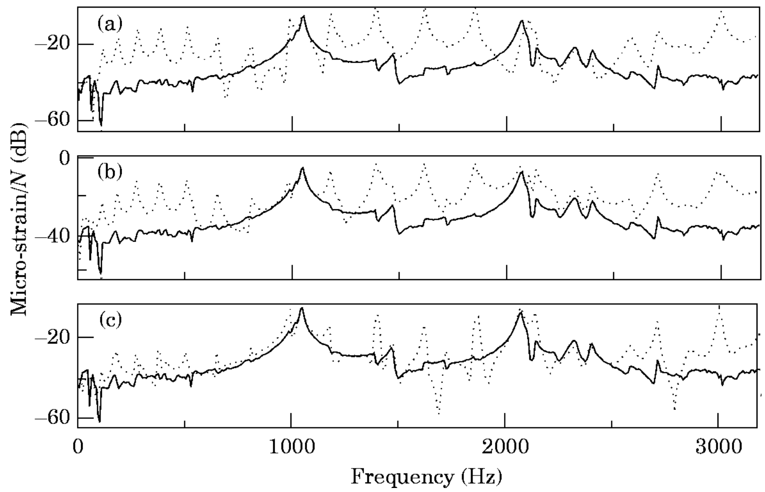

Figure 6. Decoupled FRF of longitudinal vibration at site 3. (a) Gage 3A, (b) gage 3B, (c) gage 3C; . . . . , before decoupling; ——, after decoupling.

4. DECOUPLING LONGITUDINAL AND TRANSVERSE VIBRATIONS IN THE TIME DOMAIN

By using equation (6) and (7), the time histories of longitudinal and transverse vibration of the beam at each measurement site can be separated from the measured signals at each gage. Typical decoupled results (gage 1A at site 1) in the time domain are shown in Figure 7. It is shown from the figure that the transverse vibration is more dominant than the longitudinal vibration although the beam is excited longitudinally, which makes physical sense, considering the fact that the longitudinal stiffness of the beam is much larger than its transverse stiffness.

In order to verify whether the decoupling in the time domain works as well as it does in the frequency domain, and to determine whether the decoupled signals in the time

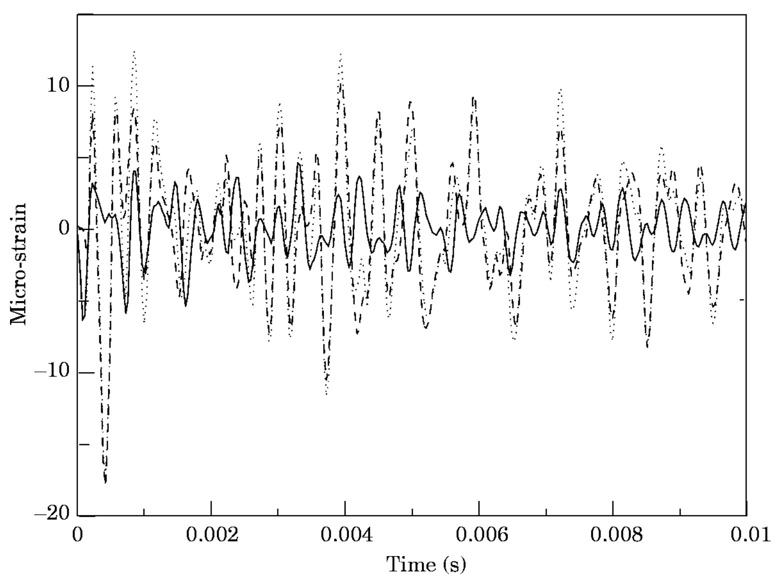

Figure 7. Typical decoupled results in the time domain: . . . . , meausred strain signal at gage 1A; ——, decoupled longitudinal vibration at site 1; – · – ·, decoupled transverse vibration at gage 1A.

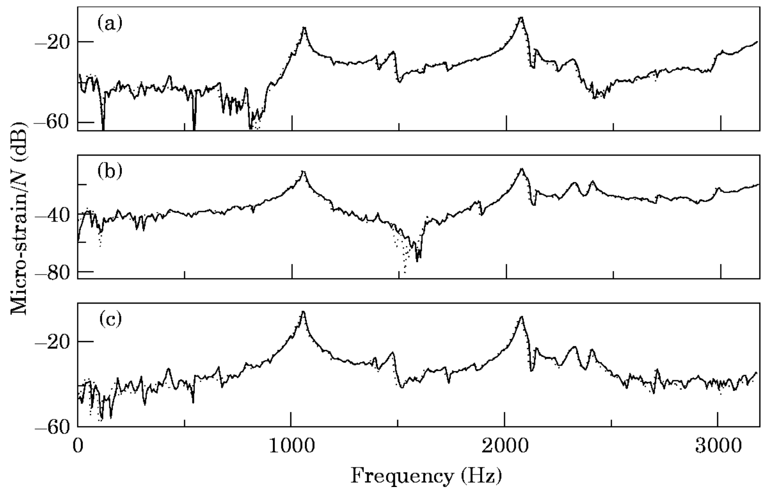

Figure 8. Comparison of calculated longitudinal FRFs with decoupled FRFs: (a) site 1, (b) site 2, (c) site 3; ——, calculated FRF based on time domain decoupling; . . . . , decoupled FRF based on FRF measurements.

domain correspond to those decoupled in the frequency domain, a Fourier transform over the decoupled time domain data was taken and the corresponding FRFs were calculated and compared. The results should be consistent with the results obtained when the signals are decoupled in the frequency domain. Figure 8 shows the comparison between the calculated FRFs of longitudinal vibration, based on the data decoupled in the time domain (equation (6)) at all three measurement sites, and the FRFs of longitudinal vibration decoupled in the frequency domain (equation (12)) based on the FRF measurements at each gage of all three sites. Figures 9–11 show the comparison between the calculated FRFs of transverse vibration using the data decoupled in the time domain (equation (7)) and the FRFs of transverse vibration decoupled in the frequency domain (equation (14)) using the FRF measurements at each gage. The comparison shows a strong consistency between the calculated FRFs and the decoupled FRFs, which implies that the time domain

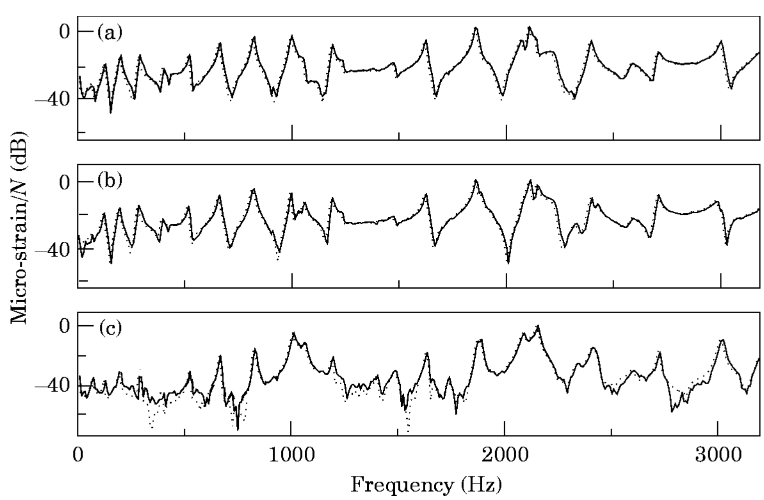

Figure 9. Comparison of calculated transverse FRFs with decoupled FRFs: (a) gage 1A, (b) gage 1B, (c) gage 1C; ——, calculated FRF based on time domain decoupling; . . . . , decoupled FRF based on FRF measurements.

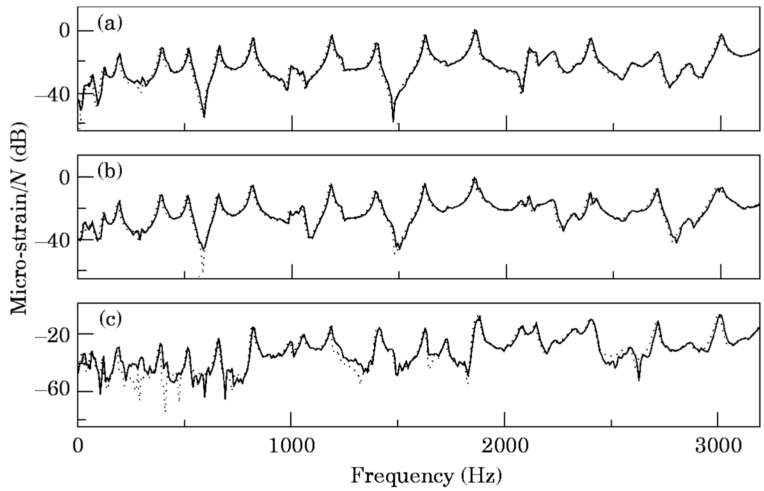

Figure 10. Comparison of calculated transverse FRFs with decoupled FRFs: (a) gage 2A, (b) gage 2B, (c) gage 2C; ——, calculated FRF based on time domain decoupling; . . . . , decoupled FRF based on FRF measurements.

decoupling works as well as in the frequency domain. The trivial and insignificant inconsistency between the calculated FRFs and the measured FRFs is mainly due to the effect of the averaging process in the FRF measurements while the calculated FRF is based only on one time history.

5. CONCLUSION

An effective method to decouple and extract both the longitudinal and the transverse vibrations of a cylindrical beam from the measurements in the time and frequency domains has been developed and presented in this paper. The approach and equations can be applied to any beam structure with a circular cross-section subjected to combined longitudinal and transverse loading. The decoupling provides a way to evaluate the

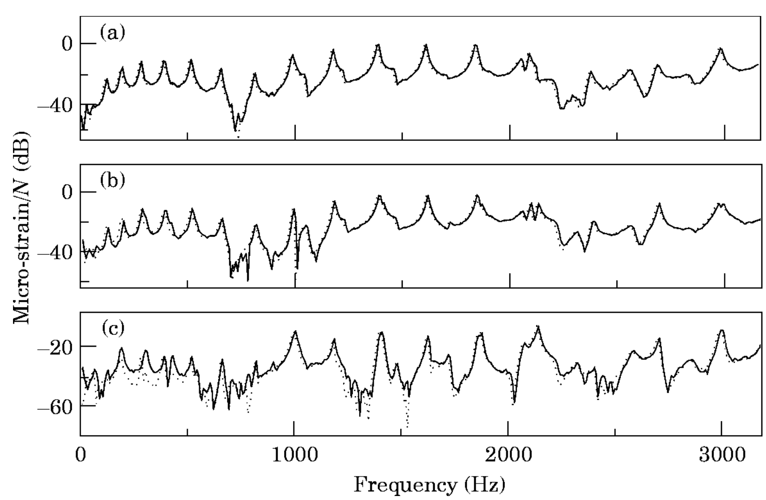

Figure 11. Comparison of calculated transverse FRFs with decoupled FRFs: (a) gage 3A, (b) gage 3B, (c) gage 3C; ——, calculated FRF based on time domain decoupling; . . . . , decoupled FRF based on FRF measurements.

significance and contribution of the longitudinal and transverse components to the total response of the beam structure. Due to the experimental set up and the layout of the strain gages, the torsional component is not sensed by the gages, and therefore has no effect on the decoupling results. It is worth noting that the quality of decoupling can be affected by the alignment of strain gages, selection and installation of the gages, and the instrumentation and data acquisition of the measurement system.

REFERENCES

1. M. E. TUTTLE 1981 *Experimental Techniques*, Society of Experimental Mechanics, 16–17. Load measurement in a cylindrical column or beam using three strain gages.
2. RICHARD HABERMAN 1987 *Elementary Applied Partial Differential Equations*. New Jersey: Prentice Hall, second edition.
3. R. SUN 1995 *Ph.D. Dissertation*, *Houghton*: *Michigan Technological University*. Analytical model and dynamic behavior of a mechanical bolt under impact.
4. R. SUN and F. O. OTUONYE 1996 *Journal of Sound and Vibration* **189**, 535–542. Effects of torque on the transverse vibration frequency of a point-anchored bolt.
5. R. B. RANDALL 1987 *Frequency Analysis*, Denmark: K. Larsen & Son, Bruel & Kjar, third edition.